ResearchGate

See discussions, stats, and author profiles for this publication at: https://www.researchgate.net/publication/44603125

Reactions of 7,8-Dithiabicyclo[4.2.1]nona-2,4-diene 7-exo-Oxide with Dodecacarbonyl Triiron Fe3(CO)12: A Novel Type of Sulfenato Thiolato Diiron Hexacarbonyl Complexes

ARTICLE *in* CHEMISTRY - AN ASIAN JOURNAL · JULY 2010

Impact Factor: 4.59 · DOI: 10.1002/asia.200900733 · Source: PubMed

CITATIONS
8

READS
32

8 AUTHORS, INCLUDING:

Ulf-Peter Apfel
Ruhr-Universität Bochum
34 PUBLICATIONS **290** CITATIONS
SEE PROFILE

Akihiko Ishii
Saitama University
251 PUBLICATIONS **2,369** CITATIONS
SEE PROFILE

Wolfgang Weigand
Friedrich Schiller University Jena
161 PUBLICATIONS **1,458** CITATIONS
SEE PROFILE

Available from: Ulf-Peter Apfel
Retrieved on: 24 January 2016

CHEMISTRY
AN ASIAN JOURNAL

DOI: 10.1002/asia.200900733

Reactions of 7,8-Dithiabicyclo[4.2.1]nona-2,4-diene 7-*exo*-Oxide with Dodecacarbonyl Triiron $Fe_3(CO)_{12}$: A Novel Type of Sulfenato Thiolato Diiron Hexacarbonyl Complexes

Jochen Windhager,[a] Ulf-Peter Apfel,[a] Tomoharu Yoshino,[b] Norio Nakata,[b] Helmar Görls,[a] Manfred Rudolph,*[a] Akihiko Ishii,*[b] and Wolfgang Weigand*[a]

Dedicated to Prof. Juzo Nakayama

Abstract: The reaction of $Fe_3(CO)_{12}$ (**13**) with 7,8-dithiabicyclo[4.2.1]nona-2,4-diene 7-*exo*-oxide (**12**) yields the sulfenato-thiolato complex **14**, which is used as starting material for further reactions. The disulfenato complex **17** is obtained by using one equivalent of dimethyldioxirane (DMD), and the monoepoxide **18** is prepared by the oxidation of **14** with an excess of DMD. Complex **14** can be converted to the monophosphine complexes **19a** and **19b** by subsequent substitution of one CO ligand using trimethylaminoxide Me_3NO and triphenylphosphine PPh_3. Additional substitution reactions are done with **17** by using acetonitrile as a ligand to form **20a** and **20b**. In the electrochemical part of the paper, the reactions of the reduced iron species **14**, **15**, **17**, and **19a** are studied.

Keywords: carbonyl ligands · electrochemistry · iron · oxidation · reduction

Introduction

The oxidative addition of cyclic disulfide compounds along the sulfur–sulfur bond to platinum(0) complexes is of current interest.[1–12] Recently, we reported the reaction of the cyclic disulfide 7,8-dithiabicyclo[4.2.1]nona-2,4-diene (**1**) with $[(Ph_3P)_2Pt(\eta^2\text{-}C_2H_4)]$ (**2**),[11] which afforded the corresponding product **3**. Interestingly, the isolated complex **3** showed a [1,5]-rearrangement to form the (dithiolato)platinum(II) complex **4** in high yields (Scheme 1).[11]

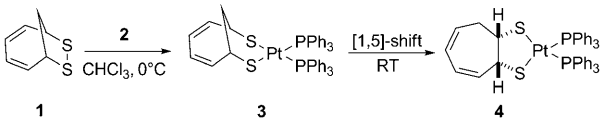

Scheme 1. [1,5]-Rearrangement of **3** to form (dithiolato)platinum(II) complex **4**.

We have also reported the oxidative addition of cyclic thiosulfinates, for example, dithiane 1-oxide **5** with **2** leading to (sulfenato-thiolato)platinum(II) complex **6** (Scheme 2).[2–7]

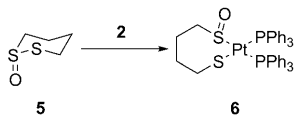

Scheme 2. Formation of (sulfenato-thiolato)platinum(II) complex **6**.

The three-membered cyclic thiosulfinates, dithiirane 1-oxides **7**, showed a similar reactivity, forming the corresponding four-membered (sulfenato-thiolato) platinum(II) complexes **8** in high yields (Scheme 3).[8,9] Alternatively, *S*-oxides of (dithiolato)platinum(II) complexes can also be prepared by photo-oxidation with molecular oxygen[13–15] or

[a] Dr. J. Windhager, U.-P. Apfel, Dr. H. Görls, Dr. M. Rudolph, Prof. Dr. W. Weigand
Institut für Anorganische und Analytische Chemie
Friedrich-Schiller-Universität Jena
August-Bebel-Strasse 2, 07743 Jena (Germany)
Fax: (+49) 3641-948102
E-mail: c8wewo@uni-jena.de

[b] T. Yoshino, Dr. N. Nakata, Prof. Dr. A. Ishii
Department of Chemistry
Graduate School of Science and Engineering
Saitama University
Saitama, Saitama 338-8570 (Japan)
Fax: (+81) 48-858-3700
E-mail: ishiiaki@chem.saitama-u.ac.jp

Supporting information for this article is available on the WWW under http://dx.doi.org/10.1002/asia.200900733.

© 2010 Wiley-VCH Verlag GmbH & Co. KGaA, Weinheim

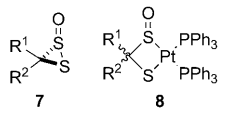

7 8

a: $R^1 = R^2$ = 1-adamantyl (1-Ad);
b: R^1 = *t*Bu, R^2 = 1-Ad;
c: R^1 = 1-Ad, R^2 = *t*Bu;
d: R^1 = Ph, R^2 = 1-Ad;
e: R^1 = H, R^2 = 9-triptycyl;

Scheme 3. Dithiirane 1-oxides **7** and their corresponding Pt^{II} complexes **8**.

by oxidation with H_2O_2.[15] Recently, we have investigated the reactions of 1,2,4-trithiolanes with platinum(0) complexes leading to the insertion of the platinum(0) complex fragment along the S–S bond.[16] Song et al. and we have also shown that the 1,2,4-trithiolane **9** can be added oxidatively to $Fe_2(CO)_9$ to give the diiron sulfur dithiolato (SDT) complex $Fe_2(\mu\text{-}SCH_2SCH_2S\text{-}\mu)(CO)_6$ **10** as well as $Fe_2(\mu\text{-}SCH_2S\text{-}\mu)(CO)_6$ **11** (Scheme 4).[17,18]

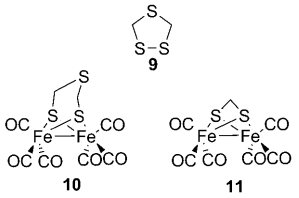

9 10 11

Scheme 4. 1,2,4-Trithiolane **9**, SDT complex **10**, and methylene dithiolato complex **11**.

These types of complexes gained the interest of researchers ever since the first X-ray structure determination of the [FeFe] hydrogenase was published,[19] and numerous model compounds suitable as models of the enzyme, such as propanedithiolato (PDT) diiron derivatives,[20a–g] azadithiolato (ADT) diiron derivatives,[20h–j] and the oxadithiolato (ODT) diiron derivatives, were synthesized (Scheme 5).[20h,l,o]

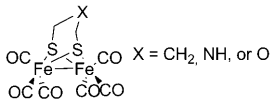

Scheme 5. PDT (X=CH_2), ADT (X=NH), and ODT (X=O) model complexes for the hydrogenase's active site.

Recently, we described the oxidation of the SDT molecule **10** and derivatives with dimethyldioxirane (DMD).[21] This initial experiment was followed by the work of Darensbourg and co-workers who figured out a possible poisoning of the enzyme by the oxidation of the sulfur atoms and a plausible repair mechanism.[22] In this paper, we report on the reaction of 7,8-dithiabicyclo[4.2.1]nona-2,4-diene 7-*exo*-oxide (**12**) and the *S*-oxide of **1** with $Fe_3(CO)_{12}$ (**13**), and we describe the reactions of the product with different equivalents of DMD as the oxidizing agent, as well as the substitution of one CO ligand by triphenylphosphine or acetonitrile. Considering its versatile functionalities (e.g., dithiolane *S*-oxide and butadiene moieties), **12** could be an interesting precursor for the synthesis of novel model complexes of the [FeFe]-hydrogenase's active site. A couple of years ago, Shaver et al.[23] and Lorenz and co-workers[24] described the syntheses of diiron hexacarbonyl complex **A** containing the 4,6-cycloheptadiene-1,3-dithiolato ligand, and complex **B** showing a (3,5-cycloheptadiene-1,2-dithiolato) moiety, respectively (Scheme 6).

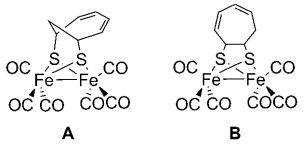

A B

Scheme 6. 4,6-cycloheptadiene-1,3-dithiolato (**A**) and 3,5-cycloheptadiene-1,2-dithiolato (**B**) containing complexes.

Results and Discussion

Reaction of $Fe_3(CO)_{12}$ (13) with 7,8-Dithiabicyclo[4.2.1]nona-2,4-diene 7-*exo*-Oxide (12)

Treatment of $Fe_3(CO)_{12}$ (**13**) with bicyclic thiosulfinate **12** in THF for two hours under reflux afforded a mixture of compounds **14**–**16**, which were separated and isolated using column chromatography (Scheme 7). Compound **16** was confirmed by the crystallographic data.[25]

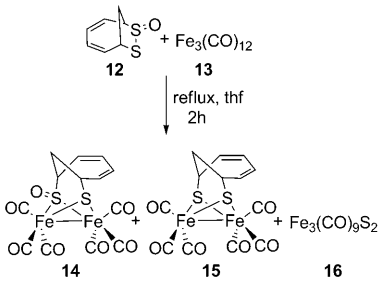

12 13 14 15 16

Scheme 7. Reaction of thiosulfinate **12** with $Fe_3(CO)_{12}$ **13**.

The IR spectrum of **14** showed the stretching vibration for νSO at 1067 cm^{-1}, which is shifted to lower frequencies compared to platinum-sulfenato metal complexes (1095–1098 cm^{-1}).[2,3,9,26] The ^1H NMR spectrum of **14** displayed eight groups of resonance signals, which were assigned to the protons H^1–H^8 (see Experimental Section). According to the ^1H–^1H COSY and ^1H–^{13}C HSQC spectra of **14** the $^{13}C\{^1H\}$ NMR resonances at δ=27.6, 32.4, 61.0, 127.8, 131.4, 132.9, and 135.5 were attributed to the C6, C7, C1, C5, C4, C3, and C2 atoms, respectively. Desorption electron ionization (DEI)-MS revealed the $[M]^+$ ion at m/z=452 and a stepwise fragmentation of six CO groups.

Single crystal X-ray analysis revealed the proposed structure of the sulfenato-thiolato complex **14** (Figure 1), which crystallized with four crystallographically independent molecules in the elemental cell. For further discussions, we referred to molecule **14A**, which is one of the four. The Fe–Fe

 © 2010 Wiley-VCH Verlag GmbH & Co. KGaA, Weinheim

These are not the final page numbers!

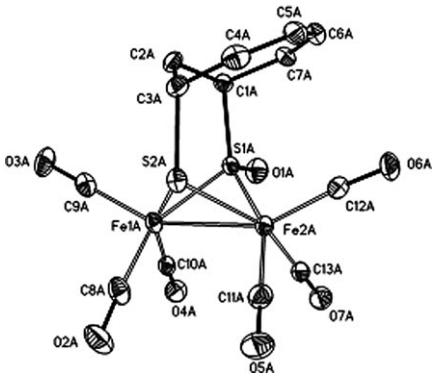

Figure 1. Molecular structure of μ,μ′-(4,6-cycloheptadiene-1-sulfenato-3-thiolato)hexacarbonyldiiron (**14 A**) with thermal ellipsoids set at the 50% probability level (hydrogen atoms are omitted for clarity). Selected distances [Å] and angles [°]: Fe(1A)–Fe(2A) 2.5370(10), Fe(1A)–C(8A) 1.795(7), Fe(1A)–C(9A) 1.819(6), Fe(1A)–C(10A) 1.789(6), Fe(1A)–S(1A) 2.1866(15), Fe(1A)–S(2A) 2.2615(16), S(1A)–C(1A) 1.847(5), S(2A)–C(3A) 1.871(5), C(4A)–C(5A) 1.343(8), S(1A)–O(1A) 1.455(4); Fe(1A)-S(1A)-Fe(2A) 70.98(5), Fe(1A)-S(2A)-Fe(2A) 68.36(4).

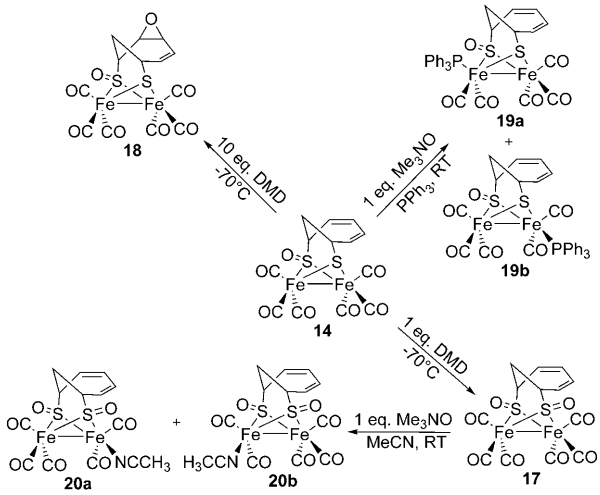

Scheme 8. Reactions of sulfenato-thiolato complex **14**.

bond length in **14A** is 2.537(1) Å, a value slightly longer than that in the unoxidized analogue **15**[23,24] (2.4974 Å). The orientation of the diene moiety is very similar to that observed in the unoxidized system: One $Fe(CO)_3$ group lies under the diene part of the ring, while the other lies under the methylene group. Interestingly, the Fe(1A)–S(1A) and Fe(2A)–S(1A) distances of 2.1866(15) and 2.1835(15) Å, respectively, were remarkably shorter than the respective Fe(1A)–S(2A) and Fe(2A)–S(2A) bond lengths, 2.2615(16) and 2.2544(14) Å. This shortening could be referred to the stronger ionic character of the SO bond.

Oxidation of the Sulfenato-thiolato Complex 14

Complex **14** was treated with one equivalent of DMD as the oxidizing agent in dichloromethane at −70 °C for five hours to afford the expected disulfenato complex **17** (Scheme 8). The IR spectrum showed the *ν*SO stretching vibration at 1059 cm^{-1}.

The ^1H NMR spectrum of **17** showed four groups of resonances, which were assigned to the diastereotopic methylene protons H^7 and H^8, the two chemically equivalent allylic protons H^1 and H^6, as well as the four olefinic protons H^2–H^5 (see Experimental Section). Interestingly, the diastereotopic protons H^7 and H^8 are strongly separated compared to those in **14**. The $^{13}C\{^1H\}$ spectrum comprised four signals arising from the methylene carbon atom ($\delta = 25.1$), the allylic carbon atoms ($\delta = 60.7$), and the two pairs of olefinic carbon atoms ($\delta = 131.9$ and 132.7). DEI-MS revealed the $[M]^+$ ion at $m/z = 468$ and a stepwise fragmentation of six CO groups.

The structure of **17** was unambiguously determined by single crystal XRD analysis (Figure 2) to be the (4,6-cycloheptadiene-1,3-disulfenato)hexacarbonyldiiron complex. The molecule showed a mirror plane. It is noticeable that the Fe–Fe bond length is 2.5562(6) Å, which is longer than

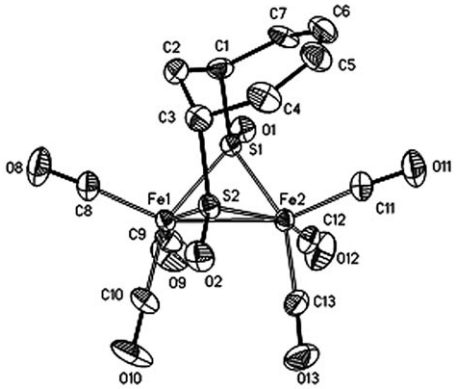

Figure 2. Molecular structure of μ,μ′-(4,6-cycloheptadiene-1,3- disulfenato)Hexacarbonyldiiron (**17**) with thermal ellipsoids set at the 50% probability level (hydrogen atoms are omitted for clarity). Selected distances [Å] and angles [°]: Fe(1)–Fe(2) 2.5562(6), Fe(1)–C(8) 1.799(4), Fe(1)–C(9) 1.791(4), Fe(1)–C(10) 1.796(4), Fe(1)–S(1) 2.1948(9), Fe(1)–S(2) 2.1929(9), S(1)–C(1) 1.846(4), S(2)–C(3) 1.851(4), C(4)–C(5) 1.335(6), S(1)–O(1) 1.483(2), S(2)–O(2) 1.485(2); Fe(1)-S(1)-Fe(2) 71.58(3), Fe(1)-S(2)-Fe(2) 71.67(3).

those in **14A** [2.5370(10) Å] and **15** (2.497 Å).[21] Likewise, we observed a shortening of the S(1)···S(2) distance from 3.027 Å in the unoxidized system **15**[23] to 2.897 Å (**14A**) and 2.808 Å (**17**) (Figure 2). As observed already in **14 A**, the Fe–S(O) bonds in the range of 2.1735–2.1948 Å are relatively short compared to the unoxidized compound **15**.[23]

The use of an excess of DMD in dichloromethane at −70 °C resulted in the formation of the *exo*-epoxide **18** (Scheme 8). ^1H and $^{13}C\{^1H\}$ NMR spectra, and XRD analysis were used to elucidate the suggested structure of **18**. The ^1H NMR spectrum of **18** exhibited seven groups of signals, which were assigned to the diastereotopic methylene protons in the range of $\delta = 2.44$–2.53, the two methine protons next to the SO groups ($\delta = 3.99/4.15$), the two protons at the epoxide ring ($\delta = 3.72/4.12$) as well as the two olefinic protons at $\delta = 6.35$ and 6.49. ^1H–^1H COSY and ^1H–^{13}C HSQC

© 2010 Wiley-VCH Verlag GmbH & Co. KGaA, Weinheim

analysis allowed the assignment of ^{13}C resonances at $\delta =$ 27.4, 54.6, 59.3, 58.7, 60.5, and 135.2/131.4 to the C7, C5, C4, C1, C6, and C2/C3, respectively (see Experimental Section). Moreover, the IR spectrum showed the νSO stretching vibration at 1055 cm^{-1} and DEI–MS revealed the $[M]^+$ ion at $m/z = 484$ and a stepwise fragmentation of six CO groups.

The single crystal diffraction analysis revealed the proposed structure of **18** and the *exo* configuration of the epoxide ring. The Fe–Fe bond length is 2.5676(7) Å, which is very similar to that in the disulfenato complex **17**. The S(1)–O(1) distance of 1.4902(18) Å is also quite similar to that in **17** [1.483(2) and 1.485(2) Å]. The epoxide ring was disordered in the crystal, and refinement was performed with occupancies of 0.5 and 0.5 for the C(3)-C(4)-O(2) ring; therefore, a discussion of the distances in the allylic epoxide moiety was not possible (Figure 3).

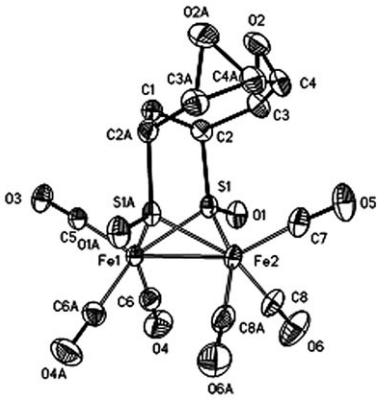

Figure 3. Molecular structure of μ,μ′-(cyclohepta-4-epoxy-6-ene-1,3-disulfenato)hexacarbonyldiiron (**18**) with thermal ellipsoids set at the 50% probability level (hydrogen atoms are omitted for clarity). Selected distances [Å] and angles [°]: Fe(1)–Fe(2) 2.5676(7), Fe(1)–C(5) 1.801(4), Fe(1)–C(6) 1.813(3), Fe(1)–S(1) 2.1899(7), Fe(2)–S(1) 2.1777(7), S(1)–C(2) 1.833(3), C(3)–C(4) 1.384(4), C(3)–O(2) 1.460(5), C(4)–O(2) 1.435(6), S(1)–O(1) 1.4902(18); Fe(1)-S(1)-Fe(2) 72.01(2).

Substitution Reactions of μ,μ'-(4,6-Cycloheptadiene-1-sulfenato-3-thiolato)hexacarbonyldiiron (14) with Triphenylphosphine

Compound **14** was reacted with one equivalent of Me_3NO in acetonitrile followed by the addition of triphenylphosphine. The reaction mixture was stirred at room temperature for one hour. After evaporation of the solvent, the crude products were redissolved in a small amount of a 1:2 mixture of THF/hexane, and compounds **19a**, **b** were isolated by using column chromatography (Scheme 8). Crystals suitable for XRD analysis were obtained by slow evaporation of the concentrated dichloromethane solutions of **19a**, **b** into hexane at 0°C. The $^{31}P\{^1H\}$ NMR spectra of the products **19a** and **19b** showed a singlet at $\delta = 60.3$ and 61.7, respectively. The IR absorption of $\nu SO = 1063$ cm^{-1} in **19a** indicated that the PPh_3 ligand has no significant electronic influence on the sulfenato moiety. However, in the case of **19b**, the νSO was observed at 1049 cm^{-1}. ^1H and $^{13}C\{^1H\}$ NMR spectra of **19a** are quite similar to those of **14**, whereas the ^1H resonance signals of the allylic protons in **19b** were remarkably shifted to higher field (**19a**: $\delta = 3.21$ and 4.38; **19b**: $\delta = 2.55$ and 3.70). Moreover, the diastereotopic protons of the methylene group were more separated in **19a** ($\Delta\delta \approx 0.5$) than those in **19b** ($\Delta\delta \approx 0.1$).

On the basis of the spectroscopic data, it was suggested that **19a** (Figure 4a) and **19b** (Figure 4b) were isomers, a result which was further confirmed by X-ray structure analysis. In complex **19a**, the PPh_3 ligand coordinated in an apical position, as visualized in Figure 4a, whereas in **19b**, the phosphine ligand showed a basal coordination (Figure 4b) according to the Fe–Fe bond. A comparison of complexes **19a** and **19b** showed that the Fe–P bond distances of 2.2484(9) Å and 2.2677(8) Å, respectively, were quite similar to the Fe–P bond distance in $Fe_2(PDT)(CO)_5PPh_3$ (2.2566(9) Å),[27a] and are similar to the values of the Fe–P bond lengths reported for PR_3-substituted diiron complexes.[20a–b,27b–g] As mentioned above, the νSO

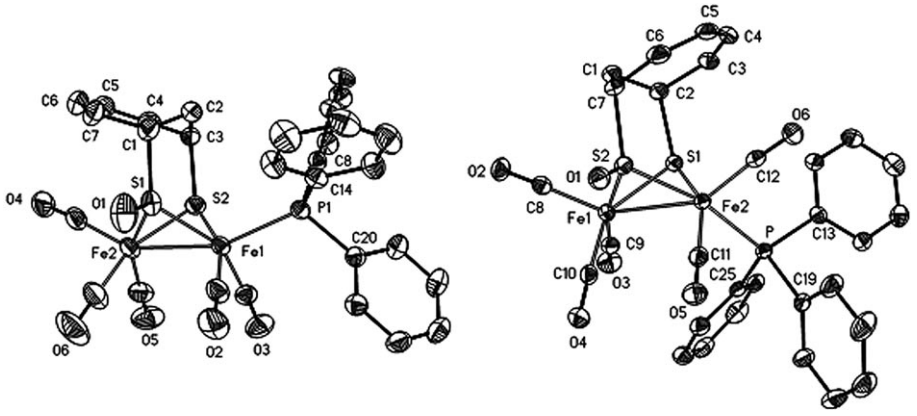

Figure 4. a) Structure of μ,μ′-(4,6-cycloheptadiene-1,3-disulfenato)(pentacarbonyl)(triphenylphosphine)diiron (**19a**) with thermal ellipsoids set at the 50% probability level (hydrogen atoms are omitted for clarity). Selected distances [Å] and angles [°]: Fe(1)–Fe(2) 2.5589(6), Fe(1)–C(26) 1.764(4), Fe(1)–C(27) 1.787(4), Fe(2)–C(28) 1.807(4), Fe(2)–C(29) 1.786(5), Fe(2)–C(30) 1.815(5), Fe(1)–S(1) 2.1927(10), Fe(1)–S(2) 2.2619(9), S(1)–C(1) 1.863(4), S(2)–C(3) 1.870(4), C(4)–C(5) 1.347(6), C(6)–C(7) 1.321(7), S(1)–O(1) 1.451(3), Fe(1)–P(1) 2.2484(9); Fe(1)-S(1)-Fe(2) 71.68(3), Fe(1)-S(2)-Fe(2) 69.11(3). b) Molecular structure of μ,μ'-(4,6-cycloheptadiene-1,3-disulfenato)(pentacarbonyl)(triphenylphosphine)diiron (**19b**) with thermal ellipsoids set at the 50% probability level (hydrogen atoms are omitted for clarity). Selected distances [Å] and angles [°]: Fe(1)–Fe(2) 2.6197(6), Fe(1)–C(8) 1.801(3), Fe(1)–C(9) 1.801(3), Fe(1)–C(10) 1.788(3), Fe(2)–C(11) 1.786(3), Fe(2)–C(12) 1.786(3), Fe(1)–S(1) 2.2387(9), Fe(1)–S(2) 2.2133(8), S(1)–C(2) 1.867(3), S(2)–C(7) 1.862(3), C(3)–C(4) 1.332(5), C(5)–C(6) 1.345(5), S(2)–O(1) 1.443(3), Fe(2)–P 2.2677(8); Fe(1)-S(1)-Fe(2) 71.77(3), Fe(1)-S(2)-Fe(2) 73.37(3).

 © 2010 Wiley-VCH Verlag GmbH & Co. KGaA, Weinheim

These are not the final page numbers!

vibration in **19b** is shifted towards lower wavenumbers, which could be explained by the basal configuration of triphenylphosphine. This configuration allowed more effective influence of the PPh_3 towards the SO moiety.

Substitution Reaction of μ,μ'-(4,6-Cycloheptadiene-1,3-disulfenato)hexacarbonyldiiron (17) with Acetonitrile

The substitution of the CO ligands in **17** by acetonitrile was explored, but the resulting products decomposed within a few minutes in solution. However, the reaction of one equivalent of Me_3NO with acetonitrile as solvent led to the stable compounds **20a** and **20b**, which were isolated by column chromatography. In the ^{1}H NMR spectrum of **20b**, the diastereotopic methylene protons gave rise to doublets of triplets ($\delta = 1.17$ and 2.24, $^2J = 14.9$ Hz, $^3J = 4.8$ Hz, $^3J = 2.7$ Hz), whereas the other protons displayed multiplets. A sharp singlet was found at $\delta = 2.24$, which was assigned to the methyl group of coordinated acetonitrile. Compared to uncoordinated acetonitrile ($\delta = 2.10$ in chloroform),[28] the resonance signal was shifted to lower field, and to higher field in $[Fe_2(S_2C_2H_4)(\mu\text{-}CO)(CO)_2(PMe_3)_3(MeCN)](PF_6)_2$ ($\delta = \sim 2.7$ in acetonitrile).[29] Also, in the $^{13}C\{^1H\}$ NMR spectrum of **20b**, the ^{13}C signals were observed at $\delta = 4.3$ and 129.6 because of the coordination of acetonitrile. Both resonances were shifted to lower field compared to the uncoordinated acetonitrile ($\delta = 1.89$ and 116.43, respectively). The ^{1}H and $^{13}C\{^1H\}$ NMR resonances of **20a** are quite similar compared to **20b.** In the IR spectra of **20a** and **20b**, we observed the νSO vibration frequency at 1054 and 1051 cm^{-1}, respectively. The νCN vibration was not identified.

The coordination of one acetonitrile in **20a** (Figure S1 in the Supporting Information) and **20b** (Figure 5) was confirmed by X-ray crystallography. In **20a**, the acetonitrile was coordinated in a basal position at Fe(1) below the cyclic diene system, whereas in **20b**, the acetonitrile is located also in basal position at Fe(2). The C≡N distance in **20b** was determined as 1.126(3) Å, the Fe(2)-N(1)-C(8) angle of 173.5(3)° and the N(1)-C(8)-C(9) angle of 176.7(3) Å were roughly linear.

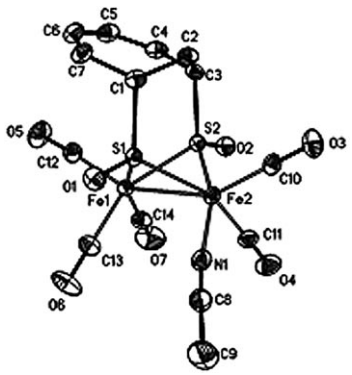

Figure 5. Molecular structure of μ,μ′-(1,3-disulfenatocyclohepta-4,6-diene)(pentacarbonyl) (acetonitrile)diiron (**20b**) with thermal ellipsoids set at the 50% probability level (hydrogen atoms are omitted for clarity). Selected distances [Å] and angles [°]: Fe(1)–Fe(2) 2.5714(5), Fe(2)–C(10) 1.792(3), Fe(2)–C(11) 1.810(3), Fe(1)–C(12) 1.785(3), Fe(1)–C(13) 1.805(3), Fe(1)–C(14) 1.804(3), Fe(1)–S(1) 2.1895(7), Fe(1)–S(2) 2.1826(7), S(1)–C(1) 1.854(3), S(2)–C(3) 1.848(2), C(4)–C(5) 1.337(4), C(6)–C(7) 1.334(4), S(1)–O(1) 1.4920(17), S(2)–O(2) 1.4861(17), Fe(2)–N(1) 1.971(2), N(1)–C(8) 1.126(3), C(8)–C(9) 1.463(4); Fe(1)-S(1)-Fe(2) 71.88(2), Fe(1)-S(2)-Fe(2) 72.91(2).

Electrochemical Investigations

To investigate the electrochemical properties of compounds **14**, **15**, **17**, and **19a**, cyclic voltammetry was performed.

High scan rates exhibit two reduction processes at −1.6 V and −2.4 V for compound **15** (Figure 6).

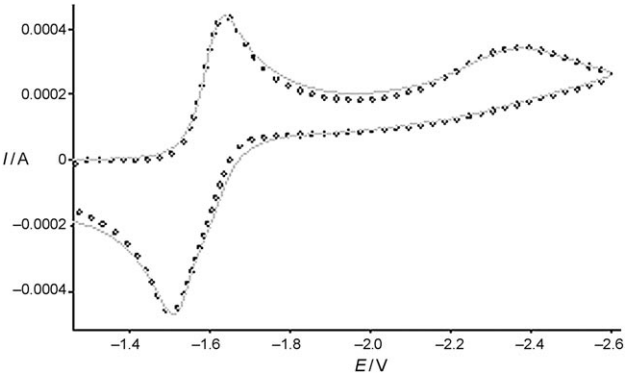

Figure 6. Comparison of the measured (thin line) and simulated CVs for the reduction of a solution of **15** in acetonitrile (0.002 M)/NBu_4PF_6 (0.25 M) (scan rate: $\nu = 150$ V s^{-1}).

Calculation of the convolution integral with $1/\sqrt{t}$ exhibits a closed loop (Figure 7). This means that the processes on the electrode can be best described by diffusion and charge-transfer processes, and no pre-equilibrium or consecutive reactions take place. The reduction occurs in two separated steps with identical peak levels, indicating two one-electron reduction steps. Derived from the analytical concentration and the electrode surface, the diffusion coefficient was determined as $D = 8.5 \times 10^{-6}$ $cm^2 mol^{-1}$ for compound **15** for

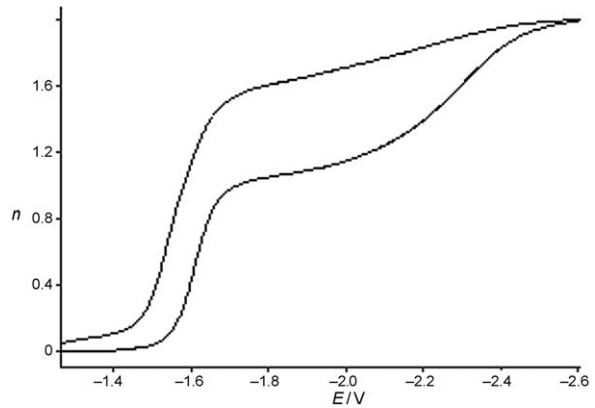

Figure 7. Convolution integral of the experimental CV of **15**.

© 2010 Wiley-VCH Verlag GmbH & Co. KGaA, Weinheim

the depicted relation between the potential and number of exchanged electrons (Figure 7). By digital simulation of the measurement, the following EE-mechanism was found in compliance to the experimental data:

$$\mathrm{Fe{-}Fe} + e \rightleftharpoons \mathrm{Fe{-}Fe^-} \quad (U_1^o = -1.610\ \mathrm{V};\ k_s^o \geq 1\ \mathrm{cm\,s^{-1}};\ D = 8.6 \times 10^{-6}\ \mathrm{cm^2\,s^{-1}}) \tag{1}$$

$$\mathrm{Fe\ Fe^-} + e \rightleftharpoons {}^-[\mathrm{Fe\ Fe}]^- \quad (U_2^o = -1.7\ \mathrm{V};\ k_s^o \approx 5.5 \times 10^{-4}\ \mathrm{cm\,s^{-1}};\ \alpha = 0.22) \tag{2}$$

In contrast to the reported complex **10**,[17b] the second reduction step appears at a more negative potential with a very small rate constant. This means, that also for compound **15**, both electron-transfer steps are chemically reversible. However, the second reduction is electrochemically irreversible and reveals a highly unsymmetric charge-transfer coefficient α. The latter is typical for processes in which a charge transfer is accompanied by significant structural changes (e.g., bond breaking, "rotated state").

The following mechanism is based on the assumption that the second reduction step is associated with the cleavage of the Fe–Fe bond, which can be regenerated during reoxidation in the back scan. However, it should be stated that this is only one possible example for a strong structural change, as this information is not accessible solely from electrochemical measurements.

The chemical reversibility of this two-step redox cycle is lost at a smaller scan rate (Figure S3 in the Supporting Information) and approximately 10% more charge is consumed for the two-electron step.

The reason for the increase of the current was not clarified unequivocally, as the enhancement of the current already starts within the potential area of the first reduction process. During measurement with smaller scan rates, a significant splitting of the reoxidation peak was observed. This splitting is only observable if the potential area of the oxidation is scanned (Figure 8).

A possible explanation was given by Talarmin and coworkers.[30] They described the possibility to form dimers of a reduced [Fe2S2] complex. A good coincidence between the experimental and the calculated cyclic voltammograms was obtained, when the following reactions were considered:

$$\mathrm{Fe{-}Fe^-} \rightarrow [\mathrm{Fe\ Fe}]^- \quad (k_3[\mathrm{P}] \approx 15) \tag{3}$$

$$\mathrm{Fe{-}Fe^-} + \mathrm{Fe{-}Fe^-} \rightleftharpoons {}^-[\mathrm{Fe{-}Fe\ Fe{-}Fe}]^- \quad (K_4 \approx 10^4;\ k_{f4} = 3.6 \times 10^3) \tag{4}$$

The fast reoxidation of the dimeric species can be seen at around −1.41 V (U_5^o) with a scan rate of 5 $\mathrm{V\,s^{-1}}$. Thereby, the regression of the monomeric iron species, Fe–Fe and Fe–Fe$^-$, afford a rate constant of approximately $8.5 \times 10^4\ \mathrm{s^{-1}}$. The rate constant of this reaction is determined by K_4, U_1^o, and U_5^o, whereby, K_4 has to be eminently larger than 1000 to afford a splitting of the signal as depicted in Figure 8. Otherwise, only the reoxidation via the Fe–Fe$^-$ species would occur, which can be very rapidly regenerated according to Equation (4). But on the other hand, K_4 is slightly larger than 10^4 as no dissociation via Equation (4) would take place, and therefore, only one electron would be needed for the iron atoms of the dimeric species. This means that the second reduction peak at around −2.2 V has to point out a much smaller endpoint ($n \leq 2$) for the convolution integral of the forward scan (Figure 7).

A good agreement between the simulated and experimental CV was obtained even at small scan rates, when the dimerization was included (Figure S3 in the Supporting Information).

However, the shape of the reoxidation between −1.3 V and −1.4 V is not displayed correctly if the potential area is increased to −2.6 V. Additionally, the reoxidation is violated at smaller scan rates ($<2\ \mathrm{V\,s^{-1}}$), and therefore can affect the shape of the experimental CV (Figure 9).

Furthermore, the electrochemical properties of compound **19a** were investigated using scan rates between 2 and 300 $\mathrm{V\,s^{-1}}$ (Figure 10).

The reduction observed at −1.75 V is chemically irreversible, and a small oxidation peak is visible at −1.35 V.

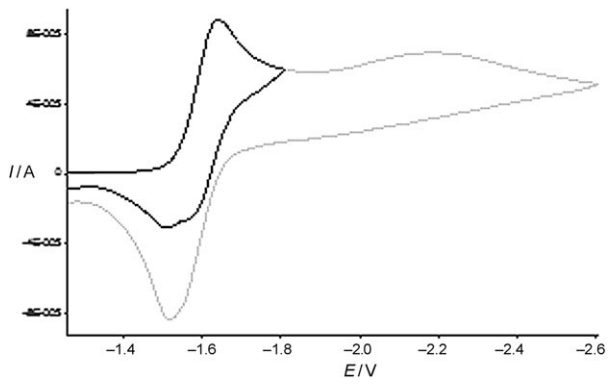

Figure 8. Reduction of a solution of **15** in acetonitrile (0.002 M)/NBu_4PF_6 (0.25 M) at a scan rate of $\nu = 5\ \mathrm{V\,s^{-1}}$.

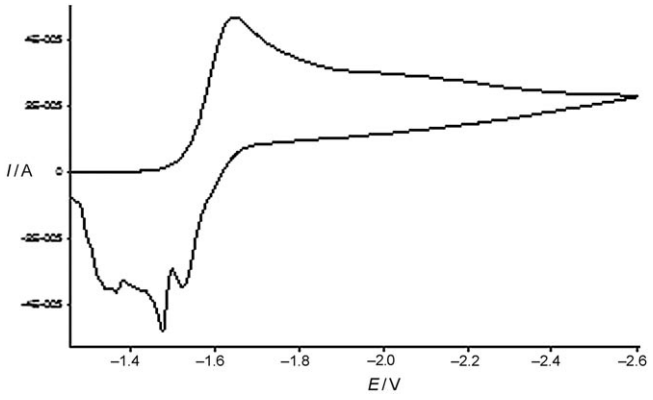

Figure 9. Reduction of a solution of **15** in acetonitrile (0.002 M)/NBu_4PF_6 (0.25 M) (scan rate: $\nu = 1\ \mathrm{V\,s^{-1}}$).

 © 2010 Wiley-VCH Verlag GmbH & Co. KGaA, Weinheim

These are not the final page numbers!

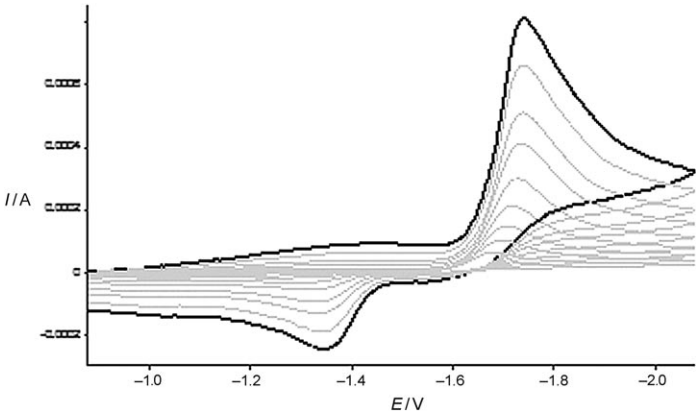

Figure 10. Reduction of **19a** (in acetonitrile (0.00173 M)/NBu_4PF_6 (0.25 M) at various scan rates: $v = 2$, 5, 10, 20, 40, 80, 120, 200, and 300 V s^{-1} (thick curve)).

Figure 11 exhibits a reversible oxidation step at −1.35 V with a related reduction peak, visible at −1.36 V. However, the linear growths of this signal with increasing scan rates reveal an adsorption process at the electrode surface.

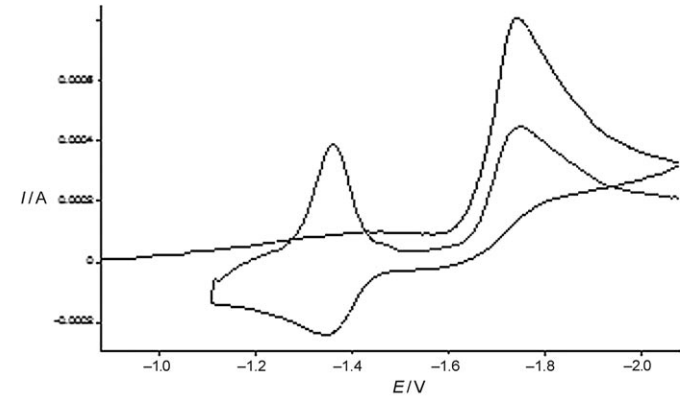

Figure 11. CV of the reduction of **19a** (in acetonitrile (0.00173 M)/NBu_4PF_6 (0.25 M); scan rate: $v = 300$ V s^{-1}).

The dependency for the reduction signal at −1.75 V between the peak current, I_p, and $\sqrt{t}$ is still linear. This confirms a diffusion-controlled reduction of **19a** and the adsorption of the reduced products. The $I_p/\sqrt{t}$- relationship affords diffusion coefficients of 2.4×10^{-5} or 3.05×10^{-6} cm^{2}s for the reduction at −1.75 V, assuming a one or two-electron transfer step. As the diffusion coefficient should not be significantly smaller than that of **15**, a useful value would be obtained for $n = 1.5$ (n = number of transferred electrons). This suggests an ECE mechanism as this would lead to a formal fractional number of transferred electrons, $1 < n < 2$. An excellent coincidence between the calculated and the experimental CV, under exclusion of adsorption processes, was found for the following reactions (see also Figure S4 in the Supporting Information):

$$\text{Fe–Fe} + e \rightleftharpoons \text{Fe–Fe}^- \ (U_1^o;\ k_{s1}^o) \quad (5)$$

$$\text{Fe–Fe}^- \rightarrow [\text{Fe Fe}]^- \ (k_2) \quad (6)$$

$$[\text{Fe Fe}]^- + e \rightleftharpoons {}^-[\text{Fe Fe}]^- \ (U_2^o;\ k_{s2}^o) \quad (7)$$

$${}^-[\text{Fe Fe}]^- \rightarrow P \ (k_4 \approx 2600\ \text{s}^-) \quad (8)$$

As the reduction of **19a** is irreversible, an almost perfect interconnection between the thermodynamic and kinetic values is observed. This is evident because of the different combinations of the rate and equilibrium constant of Equation (5)–Equation (7), and leads to the same calculated CV curves. Only the values of k_4 and the diffusion coefficient of **19a** were reproducible for all combinations. The different variations are depicted in Table 1.

Table 1. Thermodynamic and kinetic values for the theoretical CV calculations.

k_4 [s^{-1}]	U_1^o [V]	k_{s1} [cm s^{-1}]	U_2^o [V]	k_{s2} [cm s^{-1}]
10^5	−1.72	0.8	−1.725	1.1
10^6	−1.745	1	−1.72	0.5
10^7	−1.775	2	−1.72	0.45
10^8	−1.807	4	−1.72	0.45

As these combinations afford identical standard deviations for calculated and experimental CV, it is not possible to decide if the second reduction, [Eq. (7)], exhibits a more positive potential than for Equation (5). Comparison of **15** with **19a**, reveals a very fast reaction ($k_s \geq 1$ cm) for **19a** for the first reduction step with an approximately 100 mV more negative reduction potential. In the case of **15**, the reduction product is stable and can be reduced a second time in a subsequent one-electron reduction. The immense shift of about several hundred millivolts to more negative potential can be assigned mainly to kinetic overpotential, arising from the slow charge-transfer processes and structural deformation. In the case of **19a**, this structural change occurs directly after the first reduction step as a fast chemical reaction. This species has a very low stability and is reduced immediately a second time. In contrast to **15**, this two-fold reduced species is less stable and reacts in a succeeding Equation (8). A dimerization, as described in Equation (4), can be excluded because of the deviance of Equation (6).

The electrochemical properties of compounds **14** and **17** are quite similar to that of compound **19a**. In both cases, the first reduction step is irreversible, and even at higher scan rates, no reoxidation is notable (Figures 12 and 13). In the case of compound **14**, post-peaks are visible, which are possibly caused by the weak adsorption of the starting material, and probably are also an explanation for the observed shoulder (Figure 12).

The linearity between the peak current, I_p, and $\sqrt{t}$ within the potential area around −1.5 V is still valid. Assuming a diffusion coefficient similar to that of compound **15** would result in $n \approx 1.6$ and would therefore be consistent with the

© 2010 Wiley-VCH Verlag GmbH & Co. KGaA, Weinheim

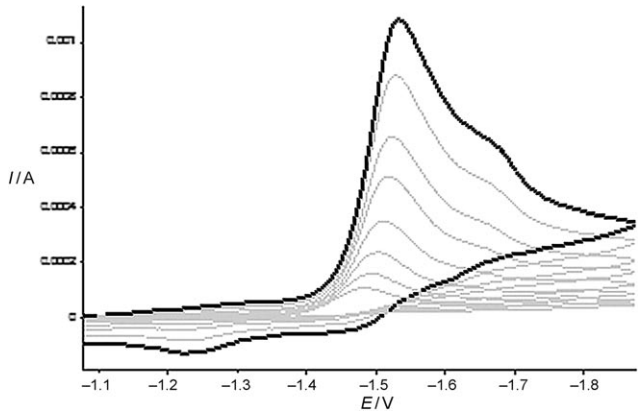

Figure 12. Reduction of a solution of **14** in acetonitrile (0.002 M)/NBu_4PF_6 (0.25 M) at scan rates: $v=5$, 10, 20, 40, 80, 120, 200, and 300 $V s^{-1}$ (thick curve).

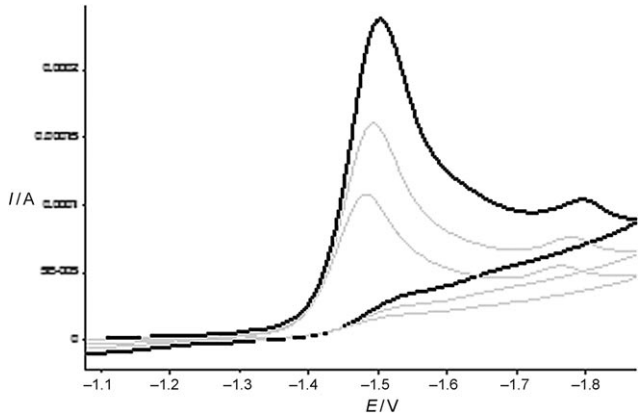

Figure 13. Reduction of **17** (in acetonitrile (0.002 M)/NBu_4PF_6 (0.25 M); scan rate: $v=5$, 10, and 20 $V s^{-1}$ (thick curve)).

results obtained for **19a**. This behavior could be reproduced by the calculated CV's. However, the standard deviation of the experimental and calculated curves was higher than for **19a**, and calculation led to different values for the diffusion coefficient. Therefore, no values are given. In analogy to **19a**, the electrochemistry of **17** has to be discussed. In contrast to compound **14**, the peak potential of the reduction is shifted about 165 mV to a more positive potential.

Conclusions

In this paper, we have investigated the coordination properties of 7,8-dithiabicyclo[4.2.1]nona-2,4-diene 7-*exo*-oxide (**12**) with $Fe_3(CO)_{12}$ (**13**) yielding the diiron compound **14**. The oxidation reaction of **14** with one equivalent of DMD led to the disulfenato complex **17**. With an excess of DMD, the monoepoxide complex **18** was obtained. The reactivity of **18** will be explored in the future. Furthermore, we have studied substitution reactions using one equivalent of Me_3NO reagent. Thus, we are able to prepare the monophosphine compounds **19a** and **19b** starting with **14**, as well as the monoacetonitrile complexes **20a** and **20b** using **17**. In accordance to digital simulation, cyclic voltammetry of compounds **14**, **15**, **17**, and **19a** exhibit different reduction mechanisms for the sulfenato-complexes and the thiolato complexes, suggesting a nonneglectable change of geometry during reduction, and a tremendous influence of the sulfenato groups arising from a diminished electron density of the [2Fe2S] cluster.

Experimental Section

General

THF was dried over KOH and distilled from sodium/benzophenone. Dichloromethane was dried over KOH and distilled from CaH_2. Acetonitrile was dried over molecular sieve (3 Å). Chemicals were received from Fluka or Acros and used without further purification. All reactions were carried out under an argon atmosphere. Thin layer chromatography (TLC) was performed on Merck silica gel 60 F_{254} plates (detection under UV light at 254 nm) and silica gel chromatography on Fluka silica gel 60. The melting points were determined on a Mel-Temp capillary tube apparatus and were uncorrected. ^1H, ^{13}C, and ^{31}P NMR spectra were determined on Bruker DRX400 (400, 100.7, and 162 MHz, respectively) spectrometers using $CDCl_3$ as the solvent at 25 °C, unless otherwise noted. IR spectra were taken on a Perkin–Elmer System 2000 FTIR spectrometer. Mass spectrometric studies (DIE-MS) were performed on a SSQ710 Finnigan MAT spectrometer. Elemental analysis was performed by the Chemical Analysis Center of Saitama University. Disulfide **1** and thiosulfinate **12** were prepared according to published procedures.[31] An acetone solution of dimethyldioxirane (DMD) was prepared by oxidation of acetone with oxone® (Sigma–Aldrich).[32,33]

*Reaction of Thiosulfinate **12** with $Fe_3(CO)_{12}$ (**13**)*

A mixture of **12** (72 mg, 0.416 mmol), $Fe_3(CO)_{12}$ **13** (209 mg, 0.415 mmol), and THF (23 mL) was stirred at reflux for 2 h. The resulting dark-brown mixture was concentrated to dryness in vacuo, and the residue was separated by silica gel chromatography using Et_2O/hexane (1:1) as the eluent. The sulfenato-thiolato complex **14** (85 mg, 45%) and dithiolato complex **15**[21,22] (28 mg, 15%) were obtained as brown crystals. **14**: $R_f=0.25$ (Et_2O/Hexane, 1:1); m.p.: 143–144 °C; IR (KBr): $\tilde{\nu}=2075$, 2035, 2023, 1998 (CO), 1067 cm^{-1} (SO); ^1H NMR ($CDCl_3$): $\delta=1.55$ (dt, $^2J_{H(7)H(8)}=15.7$ Hz, $^3J_{H(7/8)H(1)}=1.9$ Hz, 1H; $H^{7/8}$), 2.05 (dtt, $^2J_{H(7)H(8)}=15.7$ Hz, $^3J_{H(7/8)H(6)}=4.0$ Hz, $^3J_{H(7/8)H(1)}=1.9$ Hz, 1H; $H^{7/8}$), 3.32 (dtt, $^3J_{H(6)H(5)}=7.9$ Hz, $^3J_{H(6)H(7/8)}=4.0$ Hz, $^3J_{H(6)H(7/8)}=1.9$ Hz, 1H; H^6), 4.46 (dtt, $^3J_{H(1)H(2)}=7.9$ Hz, $^3J_{H(7/8)H(1)}=4.0$ Hz, $^3J_{H(7/8)H(1)}=1.8$ Hz, 1H; H^1), 6.15 (dd, $^3J_{H(5)H(4)}=11.4$ Hz, $^3J_{H(5)H(6)}=7.9$ Hz, 1H; H^5), 6.38 (dd, $^3J_{H(4)H(5)}=11.4$ Hz, $^3J_{H(4)H(3)}=7.9$ Hz, 1H; H^4), 6.64 (dd, $^3J_{H(3)H(2)}=11.4$ Hz, $^3J_{H(3)H(4)}=8.0$ Hz, 1H; H^3), 6.81 ppm (dd, $^3J_{H(2)H(3)}=11.4$ Hz, $^3J_{H(2)H(1)}=8.0$ Hz, 1H; H^2); ^{13}C NMR ($CDCl_3$): $\delta=27.6$ (C(6)), 32.4 (C(7)), 61.0 (C(1)), 127.8 (C(4)), 131.4 (C(3)), 132.9 (C(2)), 135.4 (C(5)), 206.4, 207.3 ppm (CO); MS (DEI, 70 eV): *m/z* (%): 452 (19) [M^+], 424 (44) [M^+-28; CO], 396 (22) [M^+-56; 2CO], 368 (60) [M^+-84; 3CO], 340 (22) [M^+-112; 4CO], 312 (42) [M^+-140; 5CO], 284 (100) [M^+-168; 6CO]; elemental analysis: calcd (%) for $C_{13}H_8Fe_2O_7S_2$ (452.0): C 34.54, H 1.78; found: C 34.81, H 1.63.

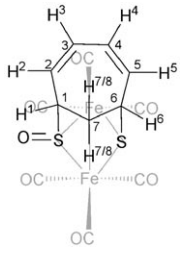

15[21,22]: $R_f=0.86$ (Et_2O/Hexane, 1:1); ^1H NMR ($CDCl_3$): $\delta=1.33$ (m, 2H, CH_2), 3.49 (m, 2H, SC*H*), 6.27 ppm (m, 4H, CH=C*H*); ^{13}C NMR ($CDCl_3$): $\delta=29.3$ (S*C*H), 32.3 (*C*H_2), 127.1, 135.5 (CH=*C*H), 206.8, 208.2 ppm (*C*O).

© 2010 Wiley-VCH Verlag GmbH & Co. KGaA, Weinheim

These are not the final page numbers!

*Oxidation of Sulfenato-Thiolato Complex **14** with DMD*

DMD (0.08 M, 1.3 mL, 0.10 mmol) was added dropwise to a solution of **14** (30 mg, 0.070 mmol) in CH_2Cl_2 (1.2 mL) under argon at −70 °C, and the mixture was stirred for 5 h at −70 to −20 °C. The resulting yellow mixture was concentrated to dryness in vacuo, and the residue was separated by silica gel chromatography using Et_2O as the eluent. The disulfenato complexes **17** (17 mg, 57 %) was obtained as yellow crystals. **17**: m.p.: 137–138 °C; IR (KBr): $\tilde{\nu}$ = 2091, 2036, 2002 (νCO), 1059 cm^{-1} (νSO); ^1H NMR ($CDCl_3$): δ = 1.33 (dt, $^2J_{H(7)H(8)}$ = 15 Hz, $^3J_{H(7/8)H(1/6)}$ = 2.7 Hz, 1H; $H^{7/8}$), 2.29 (dtt, $^2J_{H(7)H(8)}$ = 15 Hz, $^3J_{H(7/8)H(1/6)}$ = 4.8 Hz,1H; $H^{7/8}$), 4.31 (dtt, $^3J_{H(1/6)H(2/5)}$ = 6.4 Hz, $^3J_{H(1/6)H(7/8)}$ = 4.8 Hz, $^3J_{H(1/6)H(7/8)}$ = 2.7 Hz, 2H; H^1 and H^6), 6.71–6.82 ppm (m, 4H; H^{2-5}); ^{13}C NMR ($CDCl_3$): δ = 25.1 (C(7)), 60.6 (C(1) and C(6)), 131.9 (C(3) and C(4)), 132.7 (C(2) and C(5)), 206.5 ppm (CO); MS (DEI, 70 eV): *m*/*z* (%): 468 (11) [M^+], 440 (20) [M^+ −28; CO], 412 (18) [M^+ −56; 2CO], 384 (55) [M^+ −84; 3CO], 356 (9) [M^+ −112; 4CO], 328 (11) [M^+ −140; 5CO], 300 (62) [M^+ −168; 6CO]; elemental analysis: calcd (%) for $C_{13}H_8Fe_2O_8S_2$ (467.90): C 33.36, H 1.72; found: C 33.42, H 1.63.

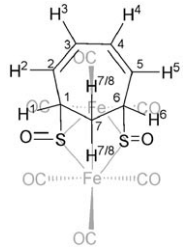

*Oxidation of Sulfenato-Thiolato Complex **14** with excess DMD*

DMD (0.08 M, 13 mL, 1 mmol) was added dropwise to a solution of **14** (30 mg, 0.070 mmol) in CH_2Cl_2 (1.2 mL) under argon at −70 °C, and the mixture was stirred for 5 h at −70 to −20 °C. The resulting yellow mixture was concentrated to dryness in vacuo and the residue was washed two times with hexane. The monoepoxide complex **18** (17 mg, 99 %) was obtained as yellow crystals. **18**: m.p.: 90–91 °C; IR (KBr): $\tilde{\nu}$ = 2090, 2031, 1999 cm^{-1} (CO), 1055 (SO); ^1H NMR ($CDCl_3$): δ = 2.48 (m, 2H; $H^{7/8}$), 3.72 (m, 1H; H^5), 3.99 (m, 1H; H^1), 4.12 (m, 1H; H^4), 4.16 (m, 1H; H^6), 6.35 (m, 1H; H^3), 6.49 ppm (m, 1H; H^2); ^{13}C NMR ($CDCl_3$): δ = 27.4 (C(7)), 54.6 (C(5)), 58.7 (C(6)), 59.3 (C(4)), 60.5 (C(1)), 54.6 (C(5)), 131.4 (C(3)), 135.2 (C(2)), 205.6 ppm (CO); MS (DEI, 70 eV): *m*/*z* (%): 484 (21) [M^+], 456 (61) [M^+ −28; CO], 428 (85) [M^+ −56; 2CO], 400 (96) [M^+ −84; 3CO], 372 (58) [M^+ −112; 4CO], 344 (97) [M^+ −140; 5CO], 316 (100) [M^+ −168; 6CO]; elemental analysis: calcd (%) for $C_{13}H_8Fe_2O_9S_2$ (484.02): C 32.26, H 1.67; found: C 32.30, H 1.60.

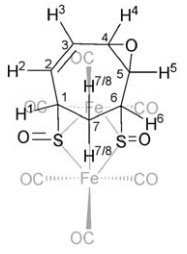

*Reaction of Sulfenato-Thiolato Complex **14** with PPh_3*

A solution of **14** (25 mg, 0.055 mmol) and PPh_3 (44 mg, 0.164 mmol) in acetonitrile (4 mL) was treated with $Me_3NO{\cdot}2H_2O$ (6 mg, 0.055 mmol) at room temperature, and the mixture was stirred for 1 h. The resulting dark-brown mixture was concentrated to dryness in vacuo, and the residue was separated by silica gel chromatography using THF/hexane (1:2) as the eluent. The PPh_3 complexes **19a** (15 mg, 40 %) and **19b** (22 mg, 58 %) were obtained as orange crystals. **19a**: R_f = 0.47 (THF/hexane, 1:2); m.p.: 123–124 °C; IR (KBr): $\tilde{\nu}$ = 2047, 2006, 1976, 1941 (CO), 1063 cm^{-1} (SO); ^1H NMR ($CDCl_3$): δ = 1.49 (m, 1H; CH_2), 2.01 (m, 1H; CH_2), 3.22 (m, 1H; SCH), 4.38 (m, 1H; SCH), 6.11 (m, 1H; CH=C*H*), 6.34 (m, 1H; CH=C*H*), 6.58 (m, 1H; CH=C*H*), 6.82 (m, 1H; CH=C*H*), 7.41–7.50 ppm (m, 15H; $P(C_6H_5)_3$); ^{13}C NMR ($CDCl_3$): δ = 29.9 (SCH), 32.4 (CH_2), 61.8 (S(O)CH), 127.3 (CH=*C*H), 128.1, 128.2, 130.3 (Ph), 131.6 (CH=*C*H), 133.0 (Ph), 133.0 (CH=*C*H), 134.0, 134.1 (Ph), 136.1 (CH=*C*H), 209.6 ppm (CO); ^{31}P NMR ($CDCl_3$): δ = 60.3 ppm; elemental analysis: calcd (%) for $C_{30}H_{23}Fe_2O_6PS_2$ (686.29): C 52.50, H 3.38; found: C 52.28, H 3.57. **19b**: R_f = 0.34 (THF/hexane, 1:2); m.p.: 124–125 °C; IR (KBr): $\tilde{\nu}$ = 2050, 1997, 1989, 1948 (CO), 1049 cm^{-1} (SO); ^1H NMR ($CDCl_3$): δ = 0.85 (m, 1H; CH_2), 1.21 (m, 1H; CH_2), 2.55 (m, 1H; SCH), 3.70 (m, 1H; SCH), 5.97 (m, 1H; CH=C*H*), 6.24 (m, 1H; CH=C*H*), 6.50 (m, 1H; CH=C*H*), 6.65 (m, 1H; CH=C*H*), 7.67–7.74 ppm (m, 15H; $P(C_6H_5)_3$); ^{13}C NMR ($CDCl_3$): δ = 27.2 (SCH), 32.0 (CH_2), 59.6 (S(O)CH), 127.4 (CH=CH), 128.7, 128.8, 130.5 (Ph), 131.0 (CH=*C*H), 133.0 (Ph), 133.0 (CH=*C*H), 133.2, 133.4 (Ph), 135.7 (CH=*C*H), 208.2 ppm (CO); ^{31}P NMR ($CDCl_3$): δ = 61.7 ppm; elemental analysis: calcd (%) for $C_{30}H_{23}Fe_2O_6PS_2$ (686.29): C 52.50, H 3.38; found: C 52.85, H 3.52.

*Reaction of Disulfenato Complex **17** with MeCN*

A solution of **17** (23 mg, 0.049 mmol) in MeCN (2 mL) was treated with $Me_3NO{\cdot}2H_2O$ (5.6 mg, 0.049 mmol) at room temperature, and the mixture was stirred for 3 h. The resulting dark-brown mixture was concentrated to dryness in vacuo, and the residue was separated by silica gel chromatography using THF/hexane (2:1) as the eluent. The MeCN complexes **20a** (9 mg, 38 %) and **20b** (8 mg, 34 %) were obtained as brown crystals. **20a**: m.p.: 103–104 °C; IR (KBr): $\tilde{\nu}$ = 2060 (CN), 2022, 1990, 1958 (CO), 1054 cm^{-1} (SO); ^1H NMR ($CDCl_3$): δ = 1.17 (m, 1H; CH_2), 2.24 (m, 1H; CH_2), 2.24 (s, 3H; CH_3), 3.97 (m, 1H; SCH), 4.33 (m, 1H; SCH), 6.58–6.88 ppm (m, 4H, CH=C*H*); ^{13}C NMR ($CDCl_3$): δ = 4.2 (CH_3), 24.9 (CH_2), 59.0 (SCH), 61.4 (S(O)CH), 128.8 (CN), 131.2, 131.6, 132.6, 133.4 (CH=*C*H), 209.0 ppm (CO); elemental analysis: calcd (%) for $C_{14}H_{11}Fe_2NO_7S_2$ (481.06): C 34.95, H 2.31, N 2.68; found: C 34.57, H 2.78, N 2.91. **20b**: m.p.: 104–105 °C; IR (KBr): $\tilde{\nu}$ = 2056 (CN), 2009, 1997, 1981 (CO), 1051 cm^{-1} (SO); ^1H NMR ($CDCl_3$): δ = 1.26 (m, 1H; CH_2), 2.33 (s, 3H; CH_3), 2.41 (m, 1H; CH_2), 3.91 (m, 1H; SCH), 4.35 (m, 1H; SCH), 6.61–6.81 ppm (m, 4H; CH=C*H*); ^{13}C NMR ($CDCl_3$): δ = 4.3 (CH_3), 25.3 (CH_2), 59.7 (SCH), 61.1 (S(O)CH), 129.6 (CN), 130.8, 131.4, 132.8, 133.2 (CH=*C*H), 208.1 ppm (CO); elemental analysis: calcd (%) for $C_{14}H_{11}Fe_2NO_7S_2$ (481.06): C 34.95, H 2.31, N 2.68; found: C 34.97, H 2.44, N 2.56.

Electrochemistry: Instrumentation and Procedures

Cyclic voltammetric measurements were conducted using a three-electrode technique with a home-built computer-controlled device based on a PCI 6110-E data acquisition board (National Instruments). The measurements were performed in acetonitrile (containing 0.25 M tetra-*n*-butylammonium perchlorate) under a blanket of solvent saturated argon. The ohmic resistance, which had to be compensated for, was determined by measuring the impedance of the system at potentials where the faradaic current was negligibly small. Background correction was accomplished by subtracting the CVs of the blank electrolyte (containing the same concentration of supporting electrolyte) from the experimental CVs. The reference electrode was an Ag|AgCl electrode in acetonitrile containing tetra-*n*-butylammonium chloride (0.25 M). As recommended by IUPAC,[34] all data reported in this paper were referenced to the ferrocenium/ferrocene couple; the measurements were taken at the end of the experiments. The working electrode was a hanging mercury drop (m = 2.79 mg) produced by a CGME instrument (Bioanalytical Systems, Inc., West Lafayette, USA). Theoretical CVs were simulated by using the DigiElch simulation package (www.DigiElch.de). The simulation algorithm used in this program has been described previously.[35] Unless otherwise stated, all charge-transfer coefficients were assumed to be 0.5.

All experimental curves were then used for finding a suitable mechanism by making use of DigiElch's nonlinear regression procedure. The standard deviation between simulated and experimental CVs was normalized with respect to the maximum peak current found in the experimental CV.

Crystal Structure Determination

X-ray structure determination of **14, 17, 18, 19a, 19b**, and **20b**: see Table 1.[36] Intensity data were collected on a Nonius Kappa CCD diffractometer using graphite-monochromated MoK_α radiation. Data were corrected for Lorentz polarization, but not for absorption effects.[37–39] Crystallographic data as well as structure solution and refinement details are summarized in Table 2.

The structures were solved by direct methods (SHELXS[39]) and refined by full-matrix least squares techniques against F_o^2 (SHELXL-97[40]). The

© 2010 Wiley-VCH Verlag GmbH & Co. KGaA, Weinheim

Table 2. Crystal data and refinement details for the X-ray structure determinations.

Compound	**14**	**17**	**18**	**19a**	**19b**	**20b**
Formula	$C_{13}H_8Fe_2O_7S_2$	$C_{13}H_8Fe_2O_8S_2$	$C_{13}H_8Fe_2O_9S_2$	$C_{30}H_{23}Fe_2O_6PS_2$	$C_{30}H_{23}Fe_2O_6PS_2$* 0.5 CH_2Cl_2	$C_{14}H_{11}Fe_2NO_7S_2$
fw [g mol^{-1}]	452.01	468.021	484.020	686.304	728.74	481.064
T [°C]	−90(2)	25(2)	25(2)	25(2)	−90(2)	25(2)
Crystal system	Triclinic	Triclinic	Monoclinic	Monoclinic	triclinic	monoclinic
Space group	P1	P1	P 2$_1$/m	P 2$_1$/c	P1	C 2/c
a [Å]	$^{-1}$13.5788(6)	8.8290(4)	8.9980(4)	11.6230(5)	10.9171(3)	22.6170(7)
b [Å]	$^{-1}$13.9037(7)	10.4400(4)	11.1790(6)	14.7900(6)	10.9276(5)	13.2080(5)
c [Å]	$^{-1}$18.3762(8)	10.4590(5)	9.5580(5)	18.8385(10)	13.2079(5)	12.8470(5)
α [°]	109.022(3)	114.393(3)	90	90	80.538(2)	90
β [°]	96.383(3)	89.679(2)	117.412(2)	103.517(2)	71.737(2)	112.189(2)
γ [°]	94.240(2)	90.363(3)	90	90	88.340(2)	90
V [Å^{-3}]	3237.1(3)	877.98(7)	853.48(7)	2973.3(2)	1475.52(10)	3553.5(2)
Z	8	2	2	4	2	8
ρ [g cm^{-3}]	1.855	1.770	1.883	1.533	1.640	1.798
μ [cm^{-1}]	20.82	19.27	19.9	12.12	13.14	19
Measured data	23112	6239	2919	18886	10590	12506
Data with I > 2σ(I)	8196	2965	1592	4832	5008	3283
Unique data/R_{int}	14680/0.0579	3325/0.020	1732/0.018	6448/0.032	6726/0.0297	3896/0.028
wR_2 (all data, on F^2)[a]	0.1278	0.1271	0.0866	0.1331	0.1102	0.0868
R_1 [$I > 2\sigma(I)$][a]	0.0569	0.0460	0.0324	0.0485	0.0419	0.0346
s[b]	0.996	1.101	1.037	1.047	1.018	1.045
Res. dens. [e·Å^{-3}]	1.256/−0.620	0.690/−0.716	0.386/−0.581	1.097/−0.730	0.489/−0.473	0.289/−0.552
Absorpt method	NONE	Multi-scan	Multi-scan	Multi-scan	NONE	multi-scan
Absorpt corr T min/max	–	0.872/0.893	0.719/0.759	0.827/0.869	–	0.740/0.830
CCDC No.	CCDC 650034	CCDC 649479	CCDC 649480	CCDC 649482	CCDC 650035	CCDC 649481

[a] Definition of the R indices: $R_1 = (\Sigma||F_o|-|F_c||)/\Sigma|F_o|$, $wR_2 = \{\Sigma[w(F_o^2-F_c^2)^2]/\Sigma[w(F_o^2)^2]\}^{1/2}$ with $w^{-1} = \sigma^2(F_o^2)+(aP)^2$.

hydrogen atoms were included at calculated positions with fixed thermal parameters. All non-hydrogen atoms except for the disordered part of molecules were refined anisotropically.[40] Only a structural motif of compound **20a** was obtained, and we will only publish the conformation of the molecule. The data was not been deposited with the Cambridge Crystallographic Data Center.

Supporting Information: Additional Figures S1–S4 briefly mentioned in the text are available in the Supporting Information. Figure S1 displays the motif of compound **20a**. Figures S2–S4 show additional electrochemical details.

Acknowledgements

Financial support for this work was provided by Japanese Society for the Promotion of Science (JSPS) and Deutscher Akademischer Austauschdienst (DAAD) (J.W.). Further support was provided by Studienstiftung des deutschen Volkes (U.-P.A.). We are grateful to Prof. Juzo Nakayama for important discussions and support.

[1] W. Weigand, S. Bräutigam, G. Mloston, *Coord. Chem. Rev.* **2003**, *245*, 167–175.
[2] W. Weigand, G. Bosl, C. Robl, W. Amrein, *Chem. Ber.* **1992**, *125*, 1047–1051.
[3] W. Weigand, R. Wünsch, *Chem. Ber.* **1996**, *129*, 1409–1419.
[4] W. Weigand, R. Wünsch, K. Polborn, G. Mloston, *Z. Anorg. Allg. Chem.* **2001**, *627*, 1518–1522.
[5] W. Weigand, R. Wünsch, C. Robl, G. Mloston, H. Nöth, M. Schmidt, *Z. Naturforsch. B* **2000**, *55*, 453–458.
[6] R. Wünsch, W. Weigand, G. Nuspl, *J. Prakt. Chem.* **1999**, *341*, 768–772.
[7] W. Weigand, R. Wünsch, K. Polborn, *Inorg. Chim. Acta* **1998**, *273*, 106–110.
[8] A. Ishii, M. Saito, M. Murata, J. Nakayama, *Eur. J. Org. Chem.* **2002**, 979–982.
[9] A. Ishii, T. Kawai, M. Noji, J. Nakayama, *Tetrahedron* **2005**, *61*, 6693–6699.
[10] A. Ishii, M. Murata, H. Oshida, K. Matsumoto, J. Nakayama, *Eur. J. Inorg. Chem.* **2003**, 3716–3721.
[11] A. Ishii, S. Kashiura, Y. Hayashi, W. Weigand, *Chem. Eur. J.* **2007**, *13*, 4326–4333.
[12] S. M. Aucott, H. L. Milton, S. D. Robertson, A. M. Z. Slawin, G. D. Walker, J. D. Woollins, *Chem. Eur. J.* **2004**, *10*, 1666–1676.
[13] Y. Zhang, K. D. Ley, K. S. Schanze, *Inorg. Chem.* **1996**, *35*, 7102–7110.
[14] W. B. Connick, H. B. Gray, *J. Am. Chem. Soc.* **1997**, *119*, 11620–11627.
[15] T. M. Cocker, R. E. Bachman, *Inorg. Chem.* **2001**, *40*, 1550–1556.
[16] a) W. Weigand, S. Bräutigam, G. Mloston, *Coord. Chem. Rev.* **2003**, *245*, 167–175 and references therein; b) T. Weisheit, H. Petzold, H. Görls, G. Mloston, W. Weigand, *Eur. J. Inorg. Chem.* **2009**, 3545–3551.
[17] a) "*11th International Symposium on Inorganic Ring Systems*" H. Petzold, S. Bräutigam, J. Windhager, W. Weigand, A. Majchrzak, G. Mloston in *Reports Series in Chemistry*, *Vol. 70* (Eds.: R. S. Laitinen, R. Oilunkaniemi) Oulu University Press, **2006**, p. 62; b) J. Windhager, M. Rudolph, S. Bräutigam, H. Görls, W. Weigand, *Eur. J. Inorg. Chem.* **2007**, *18*, 2748–2760; c) L. C. Song, Z. Y. Yang, Y. J. Hua, H. T. Wang, Y. Liu, Q.-M. Hu, *Organometallics* **2007**, *26*, 2106–2110; d) J. Windhager, H. Görls, H. Petzold, G. Mloston, G. Linti, W. Weigand, *Eur. J. Inorg. Chem.* **2007**, 4462–4471.
[18] a) A. Shaver, P. J. Fitzpatrick, K. Steliou, J. S. Butler, *J. Am. Chem. Soc.* **1979**, *101*, 1313–1315; b) C. Alvarez-Toledano, E. Delgardo, B. Donnadieu, E. Hernandez, G. Martin, F. Zamora, *Inorg. Chim. Acta* **2003**, *351*, 119–122.
[19] a) Y. Nicolet, A. L. de Lacey, X. Vernède, V. M. Fernandez, E. C. Hatchikian, J. C. Fontecilla-Camps, *J. Am. Chem. Soc.* **2001**, *123*, 1596–1601; b) Y. Nicolet, B. J. Lemon, J. C. Fontecilla-Camps, J. W. Peters, *Trends Biochem. Sci.* **2000**, *25*, 138–143; c) Y. Nicolet, C. Piras, P. Legrand, C. E. Hatchikian, J. C. Fontecilla-Camps, *Structure* **1999**, *7*, 13–23.
[20] a) X. Zhao, I. P. Georgakaki, M. L. Miller, J. C. Yarbrough, M. Y. Darensbourg, *J. Am. Chem. Soc.* **2001**, *123*, 9710–9711; b) F. Gloa-

 © 2010 Wiley-VCH Verlag GmbH & Co. KGaA, Weinheim

These are not the final page numbers!

guen, J. D. Lawrence, M. Schmidt, S. R. Wilson, T. B. Rauchfuss, *J. Am. Chem. Soc.* **2001**, *123*, 12518–12527; c) E. J. Lyon, I. P. Georgakaki, J. H. Reibenspies, M. Y. Darensbourg, *J. Am. Chem. Soc.* **2001**, *123*, 3268–3278; d) M. Razavet, S. C. Davies, D. L. Hughes, J. E. Barclay, D. J. Evans, S. A. Fairhurst, X. Liu, C. J. Pickett, *Dalton Trans.* **2003**, 586–595; e) U.-P. Apfel, Y. Halpin, H. Görls, J. G. Vos, B. Schweizer, G. Linti, W. Weigand, *Chem. Biodiversity* **2007**, *4*, 2138–2147; f) U.-P. Apfel, Y. Halpin, M. Gottschaldt, H. Görls, J. G. Vos, W. Weigand, *Eur. J. Inorg. Chem.* **2008**, *33*, 5112–5118; g) U.-P. Apfel, C. R. Kowol, Y. Halpin, F. Kloss, J. Kübel, H. Görls, J. G. Vos, B. K. Keppler, E. Morera, G. Lucente, W. Weigand, *J. Inorg. Biochem.* **2009**, *103*, 1236–1244; h) J. D. Lawrence, H. Li, T. B. Rauchfuss, M. Benard, M.-M. Rohmer, *Angew. Chem.* **2001**, *113*, 1818–1821; *Angew. Chem. Int. Ed.* **2001**, *40*, 1768–1771; i) H. Li, T. B. Rauchfuss, *J. Am. Chem. Soc.* **2002**, *124*, 726–727; j) S. Ott, M. Kritikos, B. Åkermark, L. Sun, *Angew. Chem.* **2003**, *115*, 3407–3410; *Angew. Chem. Int. Ed.* **2003**, *42*, 3285–3288; k) C. Tard, X. Liu, S. K. Ibrahim, M. Bruschi, L. De Gioia, S. C. Davies, X. Yang, L.-S. Wang, G. Sawers, C. J. Pickett, *Nature* **2005**, *433*, 610–613; l) L.-C. Song, Z.-Y. Yang, H.-Z. Bian, Q.-M. Hu, *Organometallics* **2004**, *23*, 3082–3084; m) D. Seyferth, R. S. Henderson, L.-C. Song, *Organometallics* **1982**, *1*, 125–133; n) D. Seyferth, R. S. Henderson, L.-C. Song, *J. Organomet. Chem.* **1980**, *192*, C1; o) L.-C. Song, Z.-Y. Yang, H.-Z. Bian, Y. Liu, H.-T. Wang, X.-F. Liu, Q.-M. Hu, *Organometallics* **2005**, *24*, 6126–6135; p) M. Y. Darensbourg, E. J. Lyon, J. J. Smee, *Coord. Chem. Rev.* **2000**, *206–207*, 533–561; q) R. C. Linck, T. B. Rauchfuss in *Bioorganometallics* (Ed.: D. Jaouen), Wiley-VCH, **2006**, 403–435; r) X. Zhang, C. Y. Chiang, M. L. Miller, M. V. Rampersad, M. Y. Darensbourg, *J. Am. Chem. Soc.* **2003**, *125*, 518-524; s) J. D. Lawrence, H. Li, T. B. Rauchfuss, *Chem. Commun.* **2001**, 1482–1483; t) L. C. Song, J. Gao, H. T. Wang, Y. J. Hua, H. T. Fan, X. G. Zhang, Q. M. Hu, *Organometallics* **2006**, *25*, 5724–5729.

[21] J. Windhager, R. A. Seidel, U.-P. Apfel, H. Görls, G. Linti, W. Weigand, *Chem. Biodiversity* **2008**, *5*, 2023–2041.

[22] a) T. Liu, B. Li, M. L. Singleton, M. B. Hall, M. Y. Darensbourg, *J. Am. Chem. Soc.* **2009**, *131*, 8296–8307; b) B. Li, T. Liu, M. L. Singleton, M. Y. Darensbourg, *Inorg. Chem.* **2009**, *48*, 8393–8403.

[23] A. Shaver, P. J. Fitzpatrick, K. Steliou, I. S. Butler, *J. Organomet. Chem.* **1979**, *172*, C59 - C62.

[24] A. Kramer, R. Lingnau, I.-P. Lorenz, H. A. Mayer, *Chem. Ber.* **1990**, *123*, 1821.

[25] R. Seidel, B, Schnautz, G. Henkel, *Angew. Chem.* **1996**, *108*, 1836–1839; *Angew. Chem. Int. Ed. Engl.* **1996**, *35*, 1710–1712.

[26] S. M. Aucott, P. Kilian, S. D. Robertson, A. M. Z. Slawin, J. D. Woollins, *Chem. Eur. J.* **2006**, *12*, 895–902

[27] a) P. Li, M. Wang, Ch. He, G. Li, X. Liu, Ch. Chen, B. Åkermark, L. Sun, *Eur. J. Inorg. Chem.* **2005**, 2506–2513; b) M. M. Hasan, M. B. Hursthouse, S. E. Kabir, K. M. A. Malik, *Polyhedron* **2001**, *20*, 97–101; c) R. Mejia-Rodriguez, D. Chong, J. H. Reibenspies, M. P. Soriaga, M. Y. Darensbourg, *J. Am. Chem. Soc.* **2004**, *126*, 12004–12014; d) S. Ott, M. Borgström, M. Kritikos, R. Lomoth, J. Bergquist, B. Åkermark, L. Hammarström, L. Sun, *Inorg. Chem.* **2004**, *43*, 4683–4692; e) X. Zhao, I. P. Georgakaki, M. L. Miller, R. Mejia-Rodriguez, C. Y. Chiang, M. Y. Darensbourg, *Inorg. Chem.* **2002**, *41*, 3917–3928; f) F. Gloaguen, J. D. Lawrence, T. B. Rauchfuss, M. Benard, M. M. Rohmer, *Inorg. Chem.* **2002**, *41*, 6573–6582; g) X. Zhao, C. Y. Chiang, M. L. Miller, M. V. Rampersad, M. Y. Darensbourg, *J. Am. Chem. Soc.* **2003**, *125*, 518–524.

[28] H. E. Gottlieb, V. Kotlyar, A. Nudelman, *J. Org. Chem.* **1997**, *62*, 7512–7515.

[29] J. I. van der Vlugt, T. B. Rauchfuss, S. R. Wilson, *Chem. Eur. J.* **2006**, *12*, 90–98.

[30] J.-F. Capon, F. Gloaguen, F. Y. Pètillon, P. Schollhammer, J. Talarmin, *C. R. Chim.* **2008**, *11*, 842–851.

[31] A. Ishii, S. Kashiura, H. Oshida, J. Nakayama, *Org. Lett.* **2004**, *6*, 2623–2626.

[32] W. Adam, J. Bialas, L. Hadjiarapoglou, *Chem. Ber.* **1991**, *124*, 2377.

[33] W. Adam, L. Hadjiarapoglou, A. Smerz, *Chem. Ber.* **1991**, *124*, 227–232.

[34] G. Gritzner, J. Kuta, *Pure Appl. Chem.* **1982**, *54*, 1527–1532.

[35] M. Rudolph, *J. Comput. Chem.* **2005**, *26*, 1193–1204, and references therein.

[36] CCDC 650034 (**14**), CCDC 649479 (**17**), CCDC 649480 (**18**), CCDC 649482 (**19**), CCDC 650035 (**19b**), and CCDC 649481 (**20b**) contain the supplementary crystallographic data for this paper. These data can be obtained free of charge from The Cambridge Crystallographic Data Centre at www.ccdc.cam.ac.uk/data_request/cif.

[37] COLLECT, Data Collection Software; Nonius B. V., Netherlands, **1998**.

[38] "Processing of X-Ray Diffraction Data Collected in Oscillation Mode"Z. Otwinowski, W. Minor in *Methods in Enzymology*, *Vol. 276*, *Macromolecular Crystallography*, *Part A* (Eds.: C. W. Carter, R. M. Sweet), Academic Press, New York, **1997**, pp. 307–326.

[39] G. M. Sheldrick, *Acta Crystallogr. Sect. A* **1990**, *46*, 467–473.

[40] G. M. Sheldrick, SHELXL-97 (Release 97-2), University of Göttingen, Germany.

Received: December 18, 2009
Published online: ■■ ■■, 2010

 © 2010 Wiley-VCH Verlag GmbH & Co. KGaA, Weinheim

FULL PAPERS

Oxidative Addition

J. Windhager, U.-P. Apfel, T. Yoshino, N. Nakata, H. Görls, M. Rudolph, A. Ishii,* W. Weigand** ____ ▮▮▮▮–▮▮▮▮

Reactions of 7,8-Dithiabicyclo-[4.2.1]nona-2,4-diene 7-*exo*-Oxide with Dodecacarbonyl Triiron $Fe_3(CO)_{12}$: A Novel Type of Sulfenato Thiolato Diiron Hexacarbonyl Complexes

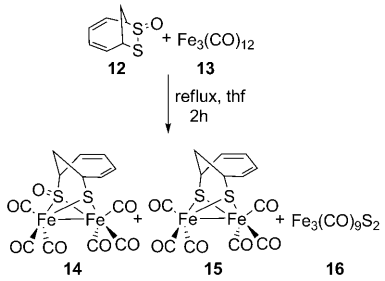

Super model! The reaction of $Fe_3(CO)_{12}$ (**13**) with 7,8-dithiabicyclo-[4.2.1]nona-2,4-diene 7-*exo*-oxide (**12**) yields the sulfenato-thiolato complex **14**, which is used as starting material for further oxidation and substitution reactions. The electrochemistry of these complexes is discussed.

 © 2010 Wiley-VCH Verlag GmbH & Co. KGaA, Weinheim

These are not the final page numbers!